RSC Advances

PAPER

View Article Online
View Journal | View Issue

Cite this: *RSC Adv.*, 2023, **13**, 21838

Green, facile and fast synthesis of silver nanoparticles by using solution plasma techniques and their antibacterial and anticancer activities†

Nguyen Van Hao, *[a] Do Hoang Tung,[b] Nguyen Phu Hung,[c] Vu Xuan Hoa,[a] Ngo Thu Ha,[c] Nguyen Thi Khanh Van,[a] Pham The Tan[d] and Pham Van Trinh *[ef]

We herein present a simple, fast, efficient and environmentally friendly method for preparing silver nanoparticles (AgNPs) using the solution plasma method in the presence of extracts from *Paramignya trimera* (*P. trimera*). The effects of *P. trimera* extract concentrations and the applied voltage on the formation of AgNPs were investigated. Surface plasmon resonance spectra show a strong peak at 413 nm for the prepared samples. The Fourier-transform infrared spectroscopy measurement results indicated the presence of possible functional groups in the prepared AgNPs. Morphological analysis revealed that the AgNPs were spherical with an average size of 8 nm. The prepared AgNPs exhibited good stability in solution compared to that of AgNPs prepared by the solution plasma technique without *P. trimera* extract. The formation mechanism of AgNPs is also proposed. The prepared AgNPs exhibited high antibacterial ability against Gram (+) *Staphylococcus aureus*, Gram (−) *Pseudomonas aeruginosa* bacteria and strong anticancer activity for the AGS gastric cancer cell line. The obtained results demonstrated that this is a simple, rapid, environmentally friendly method for preparing AgNPs instead of conventional methods using chemical reducing agents for potential applications.

Received 23rd May 2023
Accepted 13th July 2023

DOI: 10.1039/d3ra03454b

rsc.li/rsc-advances

1. Introduction

Silver nanoparticles (AgNPs) in particular are renowned for their unique optical-electrical and biological characteristics, particularly their antibacterial capabilities.[1,2] In recent years, researchers and analysts have focused on AgNPs for applications in a variety of sectors, including catalysis, optoelectronics, biomedicine, biosensors, and antibacterial activities.[3,4] Several techniques for the preparation of AgNPs such as chemical reduction and biosynthesis, and laser etching, *etc.*… have been developed and presented.[5,6] Each approach offers benefits and drawbacks in terms of cost, yield, synthesis time, solution stability and dispersion, and application purposes.[7,8] Due to the use of simple and affordable equipment, the chemical reduction approach has a high yield and is also the most preferred method for the production of AgNPs.[8,9] However, the high expense of hazardous, non-environmentally friendly chemicals, as well as rigorous control of form, size distribution, monodispersity, and purity of the preparation materials, must be taken into account. Although the biosynthesis process is environmentally favorable and low-cost, the synthesis period is lengthy and the size is difficult to manage.[10] The laser ablating approach offers a reasonably quick and clean preparation time; nevertheless, the high expense of using costly pulsed lasers, requiring a huge amount of energy, and being very laborious decreases the interest in the method.[11]

Due to their simplicity, effectiveness, cheap cost, and speed, electrochemical processes and plasma discharge have been suggested as suitable techniques for synthesizing metal nanoparticles and nanomaterials.[12–16] This is because of their simplicity, efficiency, speed, and quickness. The usage of several chemicals such as electrolytes may result in poor purity, rising manufacturing costs, and lengthy preparation times, *etc.*[12] Due to its widespread use, the plasma discharge method (plasma electrochemistry), which combines liquid phase discharge (in liquid) and gas phase discharge (in gas), is regarded as a brand-new and environmentally friendly method for the synthesis of metal nanoparticles, particularly nanosilver.[17,18]

[a]*Institute of Sciences and Technology, TNU – University of Sciences, Tan Thinh Ward, Thai Nguyen City, Vietnam. E-mail: haonv@tnus.edu.vn*
[b]*Institute of Physics, Vietnam Academy of Science and Technology, 18 Hoang Quoc Viet Str., Cau Giay Distr., Hanoi, Vietnam*
[c]*Faculty of Biotechnology, TNU – University of Sciences, Tan Thinh Ward, Thai Nguyen City, Vietnam*
[d]*Hung Yen University of Technology and Education, Khoai Chau Distr., Hung Yen Province, Vietnam*
[e]*Institute of Materials Science, Vietnam Academy of Science and Technology, 18 Hoang Quoc Viet Str., Cau Giay Distr., Hanoi, Vietnam. E-mail: trinhpv@ims.vast.vn; Tel: +84 94 319 0301*
[f]*Graduated University of Science and Technology, Vietnam Academy of Science and Technology, 18 Hoang Quoc Viet Str., Cau Giay Distr., Hanoi, Vietnam*

† Electronic supplementary information (ESI) available. See DOI: https://doi.org/10.1039/d3ra03454b

The preparation of AgNPs using the gas phase plasma discharge technique (such as microplasma, often referred to as the interaction of liquid - plasma) is typically done in air[17,19] or an inert gas medium.[20] These media frequently include stabilizers and silver salt precursors. However, because of the instability of the precursors utilized, it is challenging to regulate the production of nanoparticles using silver salts (in terms of particle shape and size). Another drawback of the microplasma approach is the very tiny contact area between the plasma jet and the precursor liquid, which results in a poor rate of metal nanoparticle generation.[20,21] By dissolving the anode in solution, plasma may be discharged in liquid to alleviate this issue. The high frequencies (a few kHz to MHz) and high voltage power supply needed for this approach, however, result in substantial input costs.[14]

The use of plant extracts as reducing agents and surface stabilizers of silver nanoparticles in green synthesis is a method of recent interest due to its environmental friendliness, simplicity and diversity.[22,23] Plant extracts derived from leaves, bark, stems, roots, fruits, seeds, and other parts of plants contain a variety of biological components such as proteins, flavonoids, aldehydes, phenols, ketones, amides, enzymes, *etc.*…[22,24–30] Recently, many previous reports have demonstrated that plant extracts with such biological components could be used as both reducing agents and surface stabilizers in the synthesis of metal nanoparticles.[24,30–33] *P. trimera* is an ethnic medicinal plant that grows in the south of Vietnam. It has traditionally been utilized for treating a variety of diseases, including cancer cells such as liver cancer, colon cancer, uterine cancer, breast cancer, and others.[34] Meanwhile, cancer is one of the leading causes of death in the world, especially in Vietnam today due to the habit of using foods containing pesticides as well as water pollution… this requires tumor-targeted solutions to minimize mortality. The use of AgNPs in the diagnosis and treatment of cancer-related diseases is attracting much attention from researchers, doctors, and pharmacists.[35] However, only a few works have investigated the anti-cancer effect of *P. trimera* extract[34] or green synthesized silver nanoparticles by other plants without any work on synthesizing AgNPs with *P. trimera* extract for antibacterial or inhibitory effects on gastric cancer cells.[36]

In this study, a new green, easy, quick, environmentally friendly, and inexpensive technique using the solution plasma method utilizing *P. trimera* extract and a high-voltage DC power supply for the synthesis of AgNPs was developed and presented for the first time. Morphological and structural studies were performed to investigate the formation mechanisms of AgNPs. In addition, we also assessed the antibacterial activity against *Staphylococcus aureus* (*S. aureus*) and *Pseudomonas aeruginosa* (*P. aeruginosa*) as well as the anticancer activity in AGS cell lines.

2. Experimental

2.1. Materials and methods

A pure silver (99.99%) rod with dimensions of 100 × 3 × 1 mm used as an electrode in the solution plasma preparation of AgNPs was bent into a L-shaped and submerged in the solution. The other electrode made by a platinum rod with a diameter of 2 mm was also immersed in the solution, the distance between the two electrodes was kept at about 0.3 mm.

P. trimera was collected from Phu Quoc National Park, Vietnam. It was washed with tap water and distilled water several times before being dried at 60 °C for 18 h in the oven. Then, *P. trimera* was cut into small pieces and made into powder and dried at 60 °C for 4 h. The extract was made from 10 g of *P. trimera* powder mixed with 150 mL of distilled water and boiled at 90 °C for 90 min. The solution was then cooled and filtered with Whatman filter paper #1 to separate the residue and obtain the extract. The final extract was stored at 4 °C in a refrigerator for gradual use.

2.2. Preparation of AgNPs by solution plasma process with *P. trimera* extract

Fig. 1 shows the installation diagram of the solution plasma system using a high-voltage DC power supply for the preparation of AgNPs with *P. trimera* extract. The plasma discharge system consists of two electrodes anode (silver rod) and a cathode (platinum rod); the reaction chamber is a 50 mL beaker; the ultrasonic tank and a DC high-voltage power supplier (5 kV) with a repetition rate of 50 Hz and a duty cycle of 50%. The process of AgNPs preparation by solution plasma method with *P. trimera* extract using high voltage DC power supply is as follows: the reaction chamber contains a 30 mL electrolyte solution including a sufficient amount of *P. trimera* extract and distilled water; insert the electrode system into the solution at a suitable distance, connect the two electrodes to a high voltage power supply, and then plasma discharge over time to obtain an AgNPs solution.

After the preparation process, the color of the solution changed from light yellow to brown, indicating the formation of AgNPs in the solution.

2.3. Characterization

The optical absorption properties of AgNPs were detected by a UV-Vis spectrometer (Jassco-V770, Japan) in the range from 250 to 800 nm. The surface morphology, particle size and elemental composition of the prepared AgNPs were determined by transmission electron microscopy and energy dispersive X-ray spectroscopy (EDS) using a JEM 1010-JEOL with an accelerating voltage of 80 kV in high contrast imaging mode. XRD analysis (X-ray diffraction) used to analyze the phase composition of AgNPs was performed using an X-ray diffractometer (D2 Rigaku) in the 2θ range of 20°–80° with Cu K_α radiation at 45 kV and current 40 mA. Fourier transform infrared absorption (FTIR) spectroscopy was used to analyze the chemical compositions and bonds of biomolecules involved in the green synthesis and stabilization of AgNPs in solution. FTIR analysis was performed using a PerkinElmer Fourier transform infrared spectrometer (Spectrum Two, USA), with a resolution of 4 cm^{-1} in the range 450–4000 cm^{-1}. Raman spectra of AgNPs (freeze-dried) samples were measured using a Horiba XploRA ONE Raman spectrometer with laser excitation at 532 nm. A fiber-optic spectrometer (AvaSpec-ULS2048, Avantes) was used to

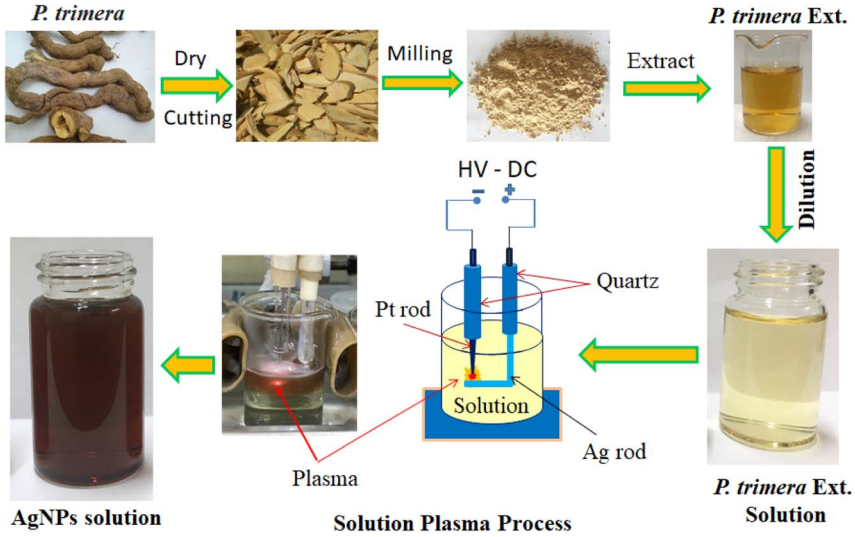

Fig. 1 Schematic diagram of the fabrication process of AgNPs by using the solution plasma technique with *P. trimera* extract.

record the optical emission spectrum (OES) of the plasma and recorded in a wavelength range of 200–900 nm and a resolution of 0.5 nm. Cell morphology was observed using phase-contrast light microscopy (Eclipse Ts2, NIKON).

2.4. Bacterial sensitivity test

The antibacterial activity of *P. trimera* extract and AgNPs prepared by the solution plasma process with *P. trimera* extract was evaluated by standard agar well diffusion method against gram (+) *S. aureus* and gram (−) *P. aeruginosa* bacteria were performed in LB broth. The bacteria were cultured in pure fresh culture on nutrient agar and incubated at 37 °C for 24 h. Nutrient agar and nutrient cultures were autoclaved for 20 min at 121 °C. The pure bacterial strain was reconstituted with a concentration of 10^6 bacteria per mL of 0.9% NaCl. Add the extract or AgNPs to wells with diameter $D = 8$ mm, each well plate a volume of 30 μL (at concentrations of 50, 25 and 12.5 μg mL^{-1}), freeze-dried. Cultural plates were incubated at 37 °C for 24 h and the diameters of inhibition zones around each well were measured by using Image J software.

2.5. Evaluation cell toxocology by MTT assay

Gastric cancer cell line AGS (RIKEN, BRC Cell Engineering Division, Japan) was used to determine cell viability when exposed to AgNPs or extract. AGS cells were cultured in Gibco RPMI 1640 medium (Gico – Thermo Fisher) in the presence of 10% fetal bovine serum and 1% penicillin/streptomycin solution (Invitrogen, Cergy-Pontoise, France) in a CO_2 incubator (5% CO_2 and 95% humidity at 37 °C).

The viability of AGS cells after treated with the extract of *P. trimera* or AgNPs was evaluated using the MTT (3-(4,5-dimethylthiazol-2)-yl)-2,5-diphenyltetrazolium bromide reagent (by Thermo Fisher). In the MTT assay, 5×10^3 cells were cultured in 96-well plates at different concentrations (5, 10, 30 and 50 mg mL^{-1}) of *P. trimera* extract and AgNPs were added to the culture medium ($n = 5$ for each concentration), in which the control samples did not contain AgNPs or *P. trimera* extracts.

After the treatment, cells were cultured for 8 h and 24 h intervals to assess cell morphology, and 10 μL per well of MTT (5 mg mL^{-1}) was added to 100 mL of fresh medium. After incubation for 4 h, the MTT solution was removed and the samples were added with 100 μL of dimethyl sulfoxide (DMSO) and incubated for 10 min at 37 °C. The optical properties of the solution were examined at an absorbance of 570 nm using a spectrophotometer plate reader (Multiskan Sky, Thermo Fisher). Cell viability was determined by the formula (1):

$$\text{Cell viability } (\%) = \frac{\text{OD}_{\text{sample}}}{\text{OD}_{\text{control}}} \times 100\% \quad (1)$$

where the OD is the optical density.

3. Results and discussion

3.1. Characteristics of AgNPs

The effects of the *P. trimera* extract concentrations and applied voltages on the formation of AgNP were investigated. Fig. 2a shows the UV-Vis absorbance spectra of AgNPs prepared with different concentration of the *P. trimera* extracts from 0.2 mL to 5.0 mL. As can be seen, the absorption peak of AgNPs prepared by the solution plasma method with *P. trimera* extract increased with the concentration of *P. trimera* extract from 0.2 mL to 3.0 mL. The spectra appeared only a single absorption peak at about 413 nm which is considered as the surface plasmon resonance peak (SPR) of AgNPs. With the higher extract concentrations of 4.0 mL and 5.0 mL, the absorption decreased and the absorption spectrum of AgNPs appeared an extra peak in the ultraviolet region at 330 nm and 327 nm. This could be due to the absorption spectrum of AgNPs being affected by the stronger interaction between AgNPs and biomolecules with high extract concentrations. In addition, the nanoparticles may be enveloped by the biomolecules of the *P. trimera* extract and/

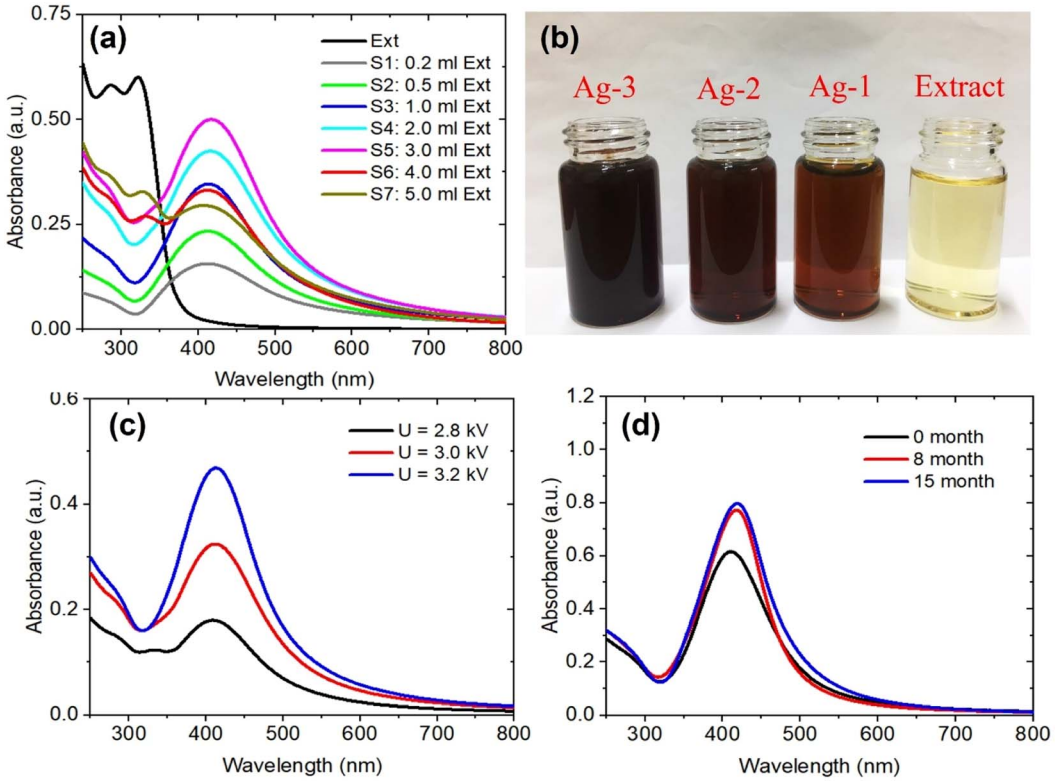

Fig. 2 UV-Vis absorbance spectra of AgNPs prepared by the solution plasma process using *P. trimera* extract (a and b) at different concentrations of *P. trimera* extracts and (c) at the different applied voltages and (d) the prepared AgNPs after quiescence for different times.

or the existence of charge clusters.[37] At a certain concentration of the *P. trimera* extract, the biomolecules presented in the extract effectively reduce Ag^+ ions to Ag^0 atoms, leading to the formation of AgNPs and also providing sufficient factors for the stability of the nanoparticles. However, with a higher extract concentration, it is possible to interfere with the plasma discharge in the solution due to the high density of biomolecules, leading to the lack of the number of Ag^+ ions and other ions (e^- and H*…) for the reduction process of Ag^+ ions to Ag^0.[38] Furthermore, when the extract concentration exceeded high, the growth of AgNPs was preferred over nucleation and agglomerated to form large particles and thus leading to a decrease in the absorbance.[38] The obtained results indicate that the appropriate *P. trimera* extract concentrations for the preparation of AgNPs were determined from 2.0 mL to 3.0 mL. The surface plasmon resonance peak at a short wavelength, a narrow absorption spectral and a quiet symmetry indicated that the prepared AgNPs have a spherical shape with small size and high stability due to the active *P. trimera* extract acting as surface functionalizing and encapsulating molecules of AgNPs. Fig. 2b shows the optical images of AgNPs prepared with different concentrations of 1.0 mL (Ag-1), 3.0 mL (Ag-2), 5.0 mL and the *P. trimera* extracts. The brown colloidal mixture formed from the solution plasma process containing the extract of *P. trimera* is visual and clear evidence of the formation of AgNPs. The brown color of the mixture after solution plasma processing can be attributed to the surface plasmon resonance of the electrons on the surface of AgNPs.[39,40] The color change in the mixture after the solution plasma process shows the formation of silver crystals from the Ag rod. Fig. 2c presents the UV-Vis absorption spectrum of AgNPs synthesized by the solution plasma method with the different applied voltages. As the voltage increased from 2.8 kV to 3.2 kV, the absorption peak becomes sharper and had higher intensity. This could be due to the rate of generation of Ag^+ ions and the density of e^- electrons in the solution increases as increasing the applied voltage, thus leading to an increase in the reduction of Ag^+ ions to AgNPs. Fig. 2d shows the UV-Vis absorption spectra of the prepared AgNPs after quiescence at different times. The obtained results indicated that, after 8 and 15 months, the absorption spectrum is nearly the same in baseline, indicating that no significant aggregation and precipitation occurred. However, the intensity of the spectrum was slightly increased and red-shifted. This could be due to the reduction of Ag^+ ions produced during plasma discharge in solution by the extract after 8 and 15 months and the growth of silver ions in the solution of nucleated AgNPs produced by previous silver nanoparticles.[41,42] As a result, the AgNPs prepared by the solution plasma method with the presence of *P. trimera* extract exhibited good stability in the solution compared to AgNPs prepared without *P. trimera* extract (ESI document†). Meanwhile, some works on the use of plant extracts as a reduction reagent to synthesize AgNPs reported that the AgNP solutions have good stability for a few days or a few months.[32,43–47] The obtained results demonstrated that

the extract of *P. trimera* is one of the most promising stabilizers among the plant extracts in the preparation of metal nanoparticles.

Morphology and particle size distribution of AgNPs were prepared by solution plasma method with *P. trimera* extract at the concentration range of the extract from 0.2 mL to 5.0 mL were observed by TEM as shown in Fig. 3. In general, the results show that the prepared AgNPs are spherical with the particle size in the range of 2–28 nm and the average particle size in the range of 8–12 nm. With the lowest concentration of *P. trimera* extract of 0.2 mL, the average size of AgNPs was about 6 nm (Fig. 3a1 and a2) and the distribution was quite wide. As shown in Fig. 3b1 and b2, at an extract concentration of 1.0 mL, the AgNPs were better dispersed and more narrowly distributed with an average particle size of about 8 nm. This indicated that, when using a small amount of extract, agglomeration is likely due to a lack of biomolecule encapsulation. As the extract was increased to a concentration of 3.0 mL, the AgNPs had more uniform dispersion in solution and also had a slightly narrower size distribution but more balanced size distribution (in the range of from 2 to 16 nm) with an average size of about 8 nm (Fig. 3c1 and c2). In this case, the nanoparticles had better separation because the surface of the nanoparticles was surrounded by biomolecules present in the extract. When the extract concentration increased higher than 3.0 mL, the nanoparticles showed a wider size distribution (from 4 to 28 nm) and the average particle size remained about 8 nm (Fig. 3d1 and d2). As the concentration of the extract increases, the molecular density of the solution increases, which can cause interference with the electrolysis of the solution. Consequently, the anode electrode corrosion is reduced, resulting in a decrease in the formation of silver atoms. This is consistent with the decrease in plasmon absorption intensity when the concentration of the extract is excessively high (Fig. 2a). The rate of reduction of Ag^{+} ions increased as the extract concentration increased, and the size distribution narrowed until the optimal concentration was 2.0–3.0 mL. This demonstrated that the extract exerts a significant effect on the formation and control of the dispersion of AgNPs in solution and their particle size distribution.

Fig. 4 shows TEM images and size distribution of AgNPs prepared by solution plasma method with *P. trimera* extract with different applied voltages of 2.8 kV, 3.0 kV and 3.2 kV; the extract concentration and plasma discharge time were kept constant at 2.0 mL and 2 min, respectively. As can be observed, the prepared AgNPs are spherical and well dispersed with the particle size distribution ranging from 4 to 24 nm. At higher voltage (at 3.2 kV), AgNPs had a narrower size distribution (Fig. 4c1 and c2), more uniform dispersion with smaller average particle size, and also higher particle density. This is also reflected in the UV-Vis absorption spectrum at 3.2 kV as the highest spectral intensity (Fig. 2c). Therefore, this is considered to be the optimal condition for the preparation of AgNPs by using the solution plasma process with *P. trimera* extract.

The biomolecules and associated functional groups that might be responsible for effective reducing and stabilizing agents of AgNPs during the solution plasma process were identified using FTIR spectroscopy. Fig. 5a presents the FTIR spectrum of the *P. trimera* extract and AgNPs at different concentrations of *P. trimera* extracts (denoted Ag-1, Ag-2 and Ag-3 respectively 1.0 mL, 3.0 mL and 5.0 mL). The results showed that the absorption bands at 3298, 1639, 1451, 1381, 1034 and 656 cm^{-1} for the *P. trimera* extract and 3359, 1638, 1384, 1035, and 642 cm^{-1} for the synthesized Ag-1; peaks at 3362, 1638, 1384, 1035, and 642 cm^{-1} for the synthesized Ag-2 and 3355, 1638, 1384, 1035, and 642 cm^{-1} for the synthesized Ag-3 (Fig. 5a). The wide bands of high intensity at 3253 and 3367 cm^{-1} correspond to the –OH stretching caused by phenolic compounds present in the *P. trimera* extract. The peaks

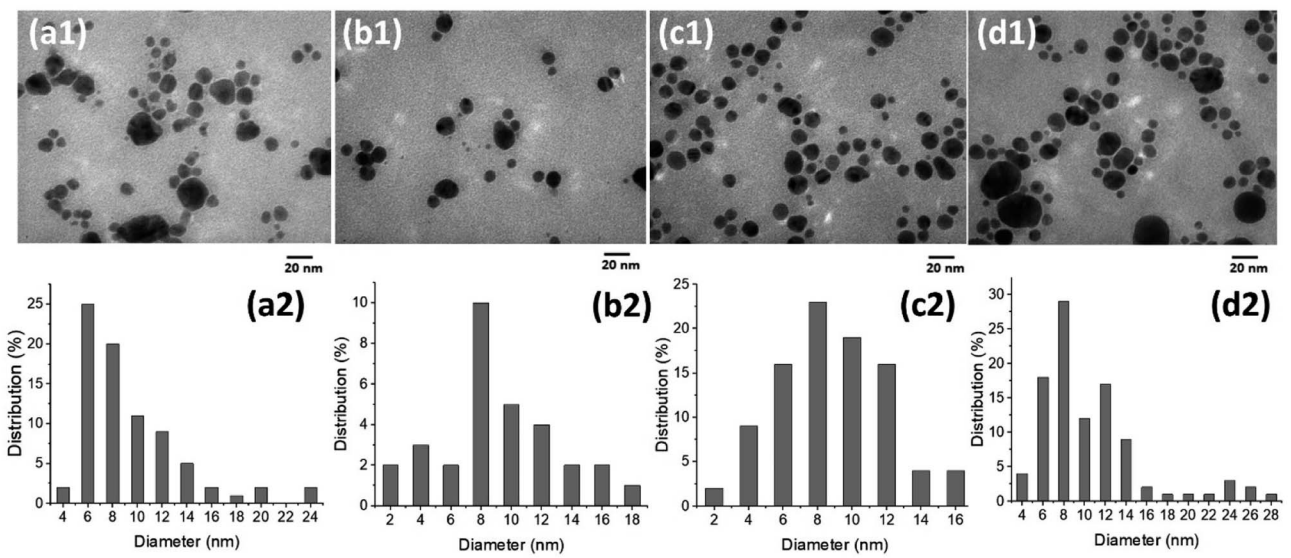

Fig. 3 TEM images and the size distribution of the AgNPs with different *P. trimera* extract concentration of 0.2 mL (a1 and a2), 1 mL (b1 and b2), 3 mL (c1 and c2) and 5 mL (d1 and d2).

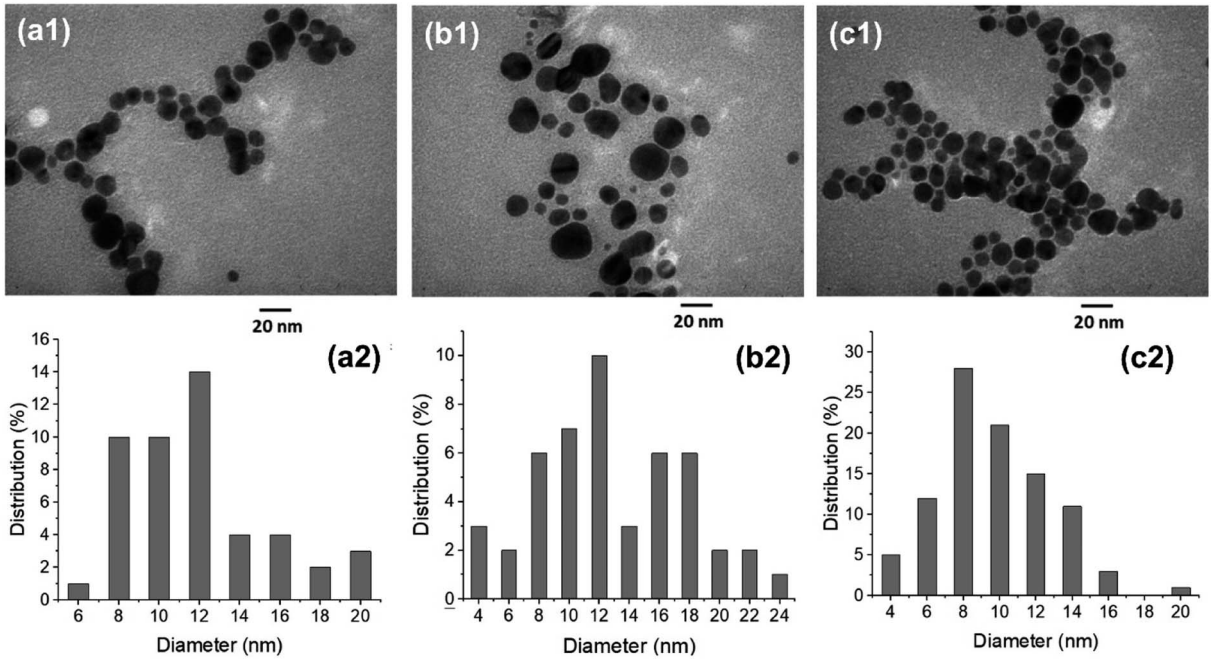

Fig. 4 TEM images and the size distribution of the AgNPs with different applied voltages of 2.8 kV (a1 and a2), 3.0 kV (b1 and b2) and 3.2 kV (c1 and c2).

appearing at 1639 cm^{-1} for *P. trimera* and 1638 cm^{-1} for AgNPs can be attributed to the C–O bond of the polysaccharide carbonyl group and the stretching oscillations of the amides that are involved in stabilizing the nanoparticles with proteins similar to previous studies.[48,49] The absorption peak appeared at wave number 1451 cm^{-1} in the FTIR spectrum of the extract of *P. trimera* and disappeared in the prepared AgNPs related to the vibration of the proteins as stabilizing agents *via* free amine groups.[50] The band at 1381–1384 cm^{-1} is attributed to the deformation of the CH_2, $-CH_3$ and C–H groups.[51] The absorption peak at nearly 1034 cm^{-1} for *P. trimera* extract and 1035 cm^{-1} for AgNPs are attributed to the C=O elongation of the alcohol groups.[52] The peaks at 642, 656, 670 and 676 cm^{-1} may be related to the alkyl halides band.[52] The spectral range from 621 to 676 cm^{-1} indicates the bending region of the aliphatic chain. The spectral peak at 1638 cm^{-1} can be attributed to the C–O bond of the polysaccharide carbonyl group and the stretching vibrations of the amides that are involved in stabilizing the nanoparticles with proteins. The absorption peak appeared at wave number 1451 cm^{-1} in the FTIR spectrum of *P. trimera* extract and disappeared in the three samples of AgNPs related to the vibration of the proteins as stabilizing agents through the free amine groups.[52] The band at 1381–1384 cm^{-1} is attributed to the deformation of the CH_2, $-CH_3$ and C–H groups.[53] To investigate in more detail the possible functional groups of the biopolymer in encapsulating and stabilizing AgNPs, Raman spectroscopy of AgNPs was recorded (Fig. 5b). As a result, the Raman spectrum of AgNPs have

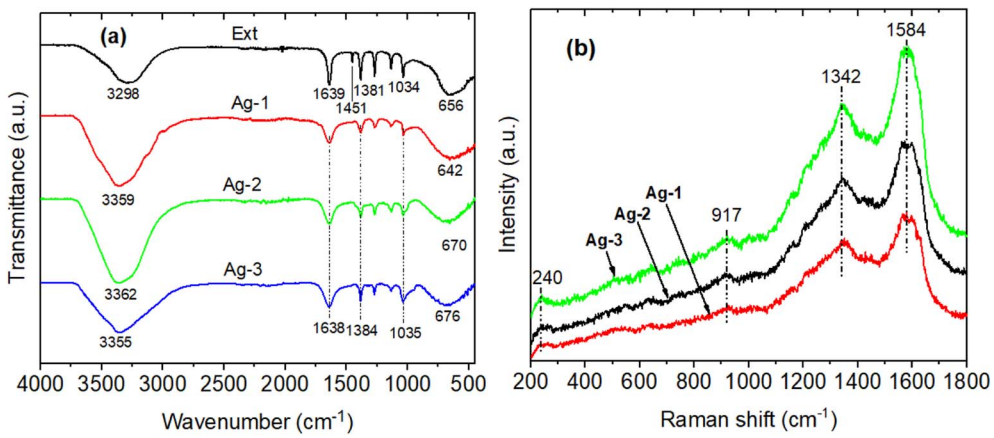

Fig. 5 (a) FTIR spectra and (b) Raman spectrum of *P. trimera* extract and AgNPs prepared by using the solution plasma process with different *P. trimera* extract concentration.

spectral peaks at 240, 917, 1342 and 1584 cm^{-1}. These peaks indicate the interaction between the extract and Ag^+ ions during solution plasma to form AgNPs.[54,55] The two wide bands at 1342 and 1584 cm^{-1} correspond to the symmetric and asymmetric C=O stretching oscillations of the carboxylate group, respectively confirming the presence of AgNPs.[56,57] The spectral peak at 240 cm^{-1} is attributed to the stretching vibration of Ag–N and Ag–O.[58–60] This peak indicated the formation of a chemical bond between silver and the amine, carboxylate groups.[56,59,60] It was also confirmed that the *P. trimera* extract encapsulates AgNPs as a surfactant.[59]

To determine the presence of AgNPs prepared by solution plasma method with *P. trimera* extract, EDS spectroscopy was performed (Fig. 6a). The obtained results indicated that the EDS spectrum has the presence of spectral peaks of Ag, C and O atoms. The spectral signal of Ag is the strongest (accounting for 78.31% by weight) and appears at about 3 keV, which is the characteristic optical absorption maximum of silver metal due to the surface plasmon resonance.[58,61] The appearance of other signals in the EDS spectrum such as C (13.6 wt%) and O (8.0 wt%) atoms could be attributed to the presence of *P. trimera* extract acting as a surface stabilizer in the preparation process. This is consistent with the results of FTIR spectral analysis related to the presence of functional groups related to the stability of silver nanoparticles synthesized by solution plasma method with *P. trimera* extract.

The crystal structures of AgNPs prepared by solution plasma method with *P. trimera* extracts at three different plasma power supply voltages were recorded using the XRD pattern (Fig. 6b) in the range of 2θ from 20° to 80°. The results show that the prepared AgNPs samples have prominent and high-intensity peaks at 2θ = 38.1°, 44.3°, 64.4° and 77.4°, respectively (111), (200), (220) and (311) Bragg reflectors of the face-centered cubic (FCC) crystal structure (JCPDS card no. 04-0783) of AgNPs, respectively. This result is consistent with the results of previous works by other authors.[62–66] The diffraction phase cleanliness of the prepared AgNPs sample clearly shows that the crystal lattice of AgNPs synthesized green by solution plasma process in combination with the extract is not affected by other molecules in the biological extract.[67]

3.2. Mechanism of the formation of AgNPs

The possible mechanism for the formation of AgNPs by the plasma discharge in the solution containing the *P. trimera* extract can be explained as follows.

3.2.1 Stage 1: electrolysis process. Initially, the plasma system acts as an electrolytic process. At the cathode occurs the electrolysis of water, in which air bubbles appear due to the hydrogen gas produced according to eqn (2):

$$2H_2O + 2e^- \rightarrow H_2 + 2OH^- \quad (2)$$

Meanwhile, at the anode, under the influence of a strong electric field, arcing effects appear in the solution plasma and the silver rod is electrolyzed. Thus, the silver at the anode will gradually dissolve (releasing Ag^+ ions) into the solution according to eqn (3):

$$Ag \rightarrow e^- + Ag^+ \quad (3)$$

When the hydrogen gas generated is large enough and the voltage is raised enough (about 2.6 kV), a continuous arc will occur. In addition, during discharge in liquids, species such as ions, electrons and neutral molecules can be generated, and their density is proportional to the discharge time.[68]

3.2.2 Stage 2: solution plasma and AgNPs formation. When voltage is applied between the anode and the cathode immersed in the solution, electrical breakdown occurs and plasma will be formed between them. The initial plasma consists of electrons, a mixture of water vapor and hydrogen ions. Since voltage is applied to the two electrodes continuously and the movement of ions is stronger, this leads to the rapid erosion of the electrode and increases the temperature of the solution.[69] Mechanism the formation of AgNPs in solution under plasma discharge between two electrodes can be divided into three regions as shown in Fig. 7a.

(i) Electrolytic zone, attracted to the anode, in which the Ag^+ ions continuously exit the silver electrode and move towards the platinum electrode.

(ii) Reduction zone: after the generation of silver ions in solution, Ag^+ can be rapidly reduced by hydrogen radicals or e^-

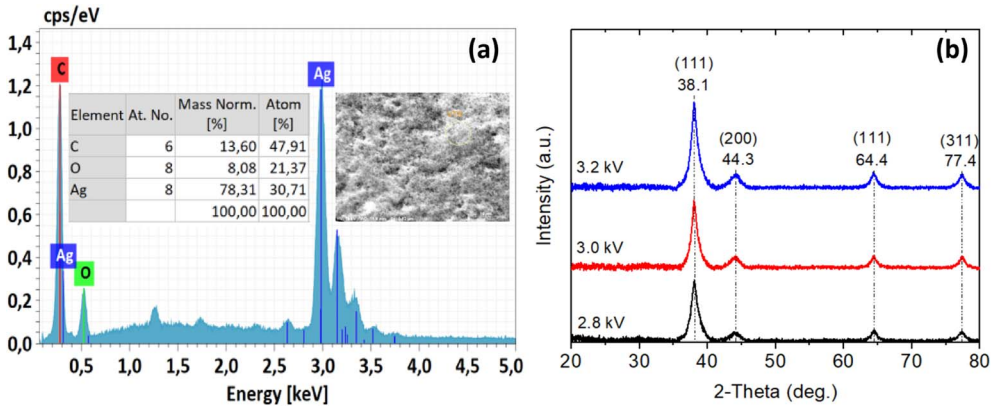

Fig. 6 The characteristics of AgNPs prepared by solution plasma method with *P. trimera* extract. (a) EDS and (b) XRD.

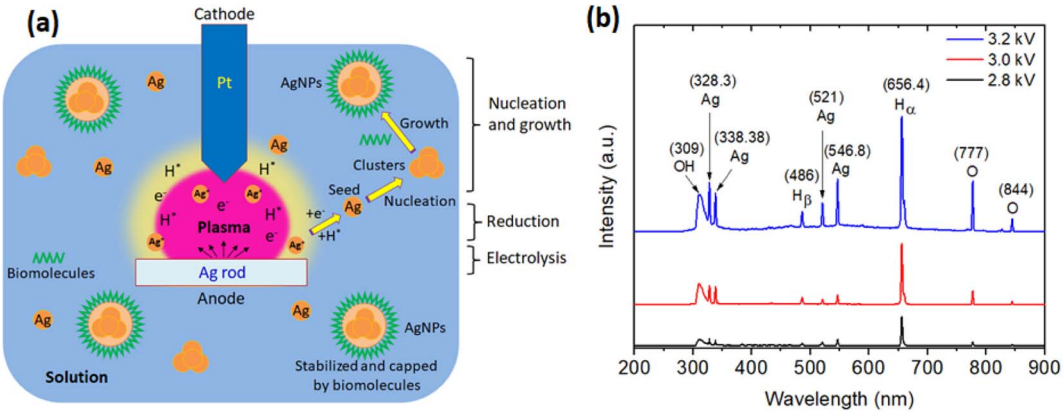

Fig. 7 (a) A Schematic illustration of the proposed mechanism of the formation of AgNPs during a solution plasma discharge and biosynthesis and (b) Optical emission spectra (OES) measured during solution plasma process with *P. trimera* extract at different applied voltages.

generated in solution plasma to form atomic silver Ag^0 as shown in eqn (4) and (5).

$$Ag^+ + H^* \rightarrow Ag + H^+ \quad (4)$$

$$Ag^+ + e^- \rightarrow Ag \quad (5)$$

by the reduction reaction, hydrogen ions are produced, which lowers the pH of the solution (eqn (4)). The heat generated during the arc discharge and the discharge medium also influences the formation of nanoparticles.[70,71] In addition, the formation of AgNPs also contributes to nucleation by hydrated electrons (e_{aq}) which act as strong reducing agents as shown in eqn (6).[72]

$$\text{Bio-molecules} + Ag^+ + e_{aq}^- \rightarrow Ag \quad (6)$$

Phenolics are aromatic rings with one or more hydroxyl groups present in the biologically active substance. The antioxidant and redox properties of phenolic compounds help to absorb and neutralize free radicals, quench single and triple groups, or decompose peroxides rapidly. It is this resonance in phenol that rapidly reduces the Ag^+ ion to a silver atom.[73]

(iii) The nucleation and growth zone, where Ag nanoparticles are formed and grown into AgNPs.

To support the proposed mechanism, the optical emission spectra (OES) were measured during the solution plasma process in the synthesis of AgNPs with the extract of *P. trimera* at different plasma power supplies. As shown in Fig. 7b, the OES of the plasma in all three cases with different applied supply voltages of 2.8 kV, 3.0 kV and 3.2 kV all include the lines from the OH radical at 309 nm, the O atom lines at 777 nm and 844 nm, and the H_β and H_α atomic hydrogen lines at 486 nm and 656.4 nm coexist in the arc-discharge solution.[14,74,75] As the applied voltage increases, the intensity of the emission lines also increases, but at the voltage of 3.2 kV, the emission peaks of Ag tend to be higher than those of OH. This indicates a larger amount of Ag is produced and it is consistent with the absorption spectrum of AgNPs at an increased applied voltage (Fig. 2c). These emission lines are all the result of the dissociation of H_2O.[75] Emissions due to excited states of Ag atoms are also observed at the 328.3 nm lines; 338.38 nm; 521 nm and 546.8 nm, however with lower intensities, indicating that Ag particles are formed during arc-discharge, where these lines are related to the transitions of Ag neutral.[75] Ag atoms are separated from the Ag electrode when bombarded by plasma species such as H, OH radicals and O atoms.

3.3. Antibacterial activity

The antibacterial properties of AgNPs were investigated against Gram (+) *S. aureus* and Gram (−) *P. aeruginosa* by using an agar-well diffusion assay, and the inhibition zone was established in Table 1 and Fig. 8.

The prepared AgNPs showed effective antibacterial activity against both Gram (−) and (+) bacteria. Silver nanoparticles prepared by plasma-solution method with *P. trimera* extract showed a maximum inhibition zone of about 31 mm for *S. aureus* and 29 mm for *P. aeruginosa* at a concentration of 50 μg mL^{-1} (denoted AgNPs-1). On the other hand, the negative control (distilled water) and *P. trimera* extract did not have any inhibition zones. At concentrations of AgNPs lower than 25 μg mL^{-1} (denoted AgNPs-2) and 12.5 μg mL^{-1} (denoted AgNPs-3) for a smaller zone of inhibition. AgNPs showed antibacterial activity against both Gram (+) and (−) bacteria, with dose-dependent antibacterial activities. The antibacterial activity of AgNPs was completely concentration-dependent, with high concentrations of AgNPs showing more inhibitory activity on

Table 1 Antimicrobial activity of AgNPs prepared by solution plasma process with *P. trimera* extract

	Zone of inhibition (diameter of mm)	
Samples	*S. aureus*	*P. aeruginosa*
AgNPs-1	31	29
AgNPs-2	26	20
AgNPs-3	24	18
Ext	0	0
H_2O	0	0

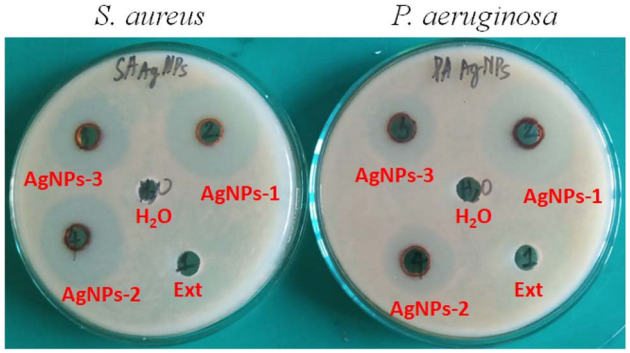

Fig. 8 Antimicrobial activity of prepared AgNPs against *S. aureus* and *P. aeruginosa*.

bacterial growth.[76] The mechanism of effective antibacterial activity of silver nanoparticles against diverse dangerous bacteria has not been understood and requires additional investigation.[77,78] There are several proposed mechanisms such as (i) generation of reactive oxygen species (ROS) including superoxide anion (O_2^-) and hydroxyl radical ($OH^•$), (ii) presence of Ag^+ ion in AgNPs form binding to sulfur- and phosphorus-containing compounds, directly leading to spontaneous reduction of the protein in bacteria[79] and (iii) the release of Ag^+ ions from AgNPs that simply enter cell wall and cause disturbances of its functions such as permeability and respiration. It is therefore evident that the binding of particles to microorganisms depends on the surface area available for entry. In general, small nanoparticles have a larger surface area, which makes it easier to penetrate bacteria than large particles, due to their greater antibacterial activity.[78–80] In this study, AgNPs with an average size of 8–10 nm easily attach to the surface of cell membranes and disturb their normal activities such as increasing permeability due to changes in cell membrane structures that lead to cell death.[81,82] The effect of AgNPs on bacteria also results in a lower inhibition zone for Gram (−) bacteria than for Gram (+) bacteria. This may be because the cell wall of Gram (−) bacteria consists of multiple layers of denser rigid peptidoglycan, as it prevents nanoparticles from entering the cell wall.[83]

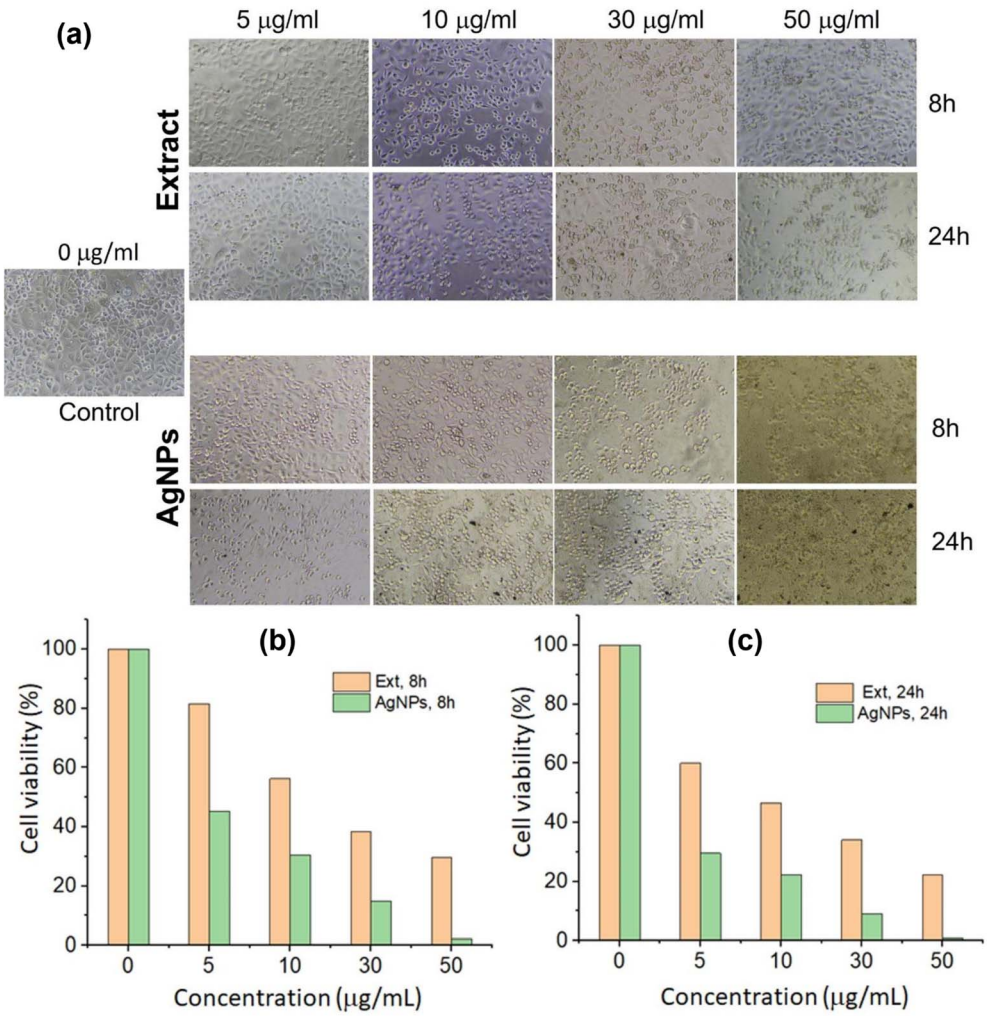

Fig. 9 Morphological observations of AGS cells treated with extracts and AgNPs at 8 h and 24 h culture intervals (a); anti-cancer effects of *P. trimera* and AgNPs on human gastric cancer cell line AGS for 8 h (b) and 24 h (c). The scale bar is 50 μm.

3.4. Anticancer activity

The anticancer activity of AgNPs samples was screened based on MTT cytotoxicity assessments in 8 h and 24 h. The MTT method is an appropriate, efficient, rapid and commonly used method because of its high reproducibility and can be used for both determinations of cell viability and cytotoxicity. Fig. 9a presents AGS cell surface morphology treated with extract and AgNPs over the 8 h and 24 h culture periods, and anticancer effects of *P. trimera* extract and AgNPs on human gastric cancer cell line AGS for 8 h (Fig. 9b) and 24 h (Fig. 9c). Observation of cell surface morphology, when treated with extract and AgNPs, can show changes in the shape of cells compared with control cells (untreated), in which, cells treated with AgNPs or *P. trimera* extract cells were broken and a few changed to a round shape (Fig. 9a).

The results also showed that both extracts and AgNPs had cytotoxic effects on AGS cells compared to the control, and the cell viability depended on both the concentration of compounds and treatment time. When the concentration of compounds is increased, their anti-cancer effect also increases. However, inhibitory effects of AgNPs synthesized by solution plasma method is higher than extract at same concentration. The IC_{50} value of AgNPs identified is 30 μg mL^{-1}, compared to 50 μg mL^{-1} in extract. In particular, the treatment of AGS cells with AgNPs synthesized by plasma method with *P. trimera* extract showed a very high inhibitory ability (~1% viability) at a concentration of 50 μg mL^{-1} while the rate of viability cells is about 30% at same concentration of the extract. In addition, the most obvious and noticeable effect after treating AGS cells with plasma-synthesized AgNPs with *P. trimera* extract was the change in cell shape. Therefore, it can be concluded that these prepared AgNPs have a significant anti-cancer effect on the gastric cell line AGS, which increases the potential application of AgNPs as anti-cancer drugs. The results of this study are comparable with previous studies on green-synthesized nanosilver with different plants in anti-cancer effect with AGS cell line.[84–86] The results also suggest a potential anticancer effect of *P. trimera* against gastric cancer cell lines. This result is similar to previous reports on the anti-cancer effect of *P. trimera* on the cell lines MCF-7, HT29, H460….[34]

The possible cytotoxic mechanism of AgNPs is attributed to the ability to generate free radicals of silver nanoparticles, which interfere with cell aggregation and induce cell death.[87,88] In addition, the interaction of AgNPs with cancer cells can induce electrons that lead to the generation of active oxygen radicals that induce cell death.[89] Moreover, similar studies also show that green synthesized nanosilver with extracts from ethnic herbs can increase the anti-cancer ability of nanoparticles through the generation of active oxygen radicals, and radicals harmful, can cause oxidative stress, mutate protein function, and destroy cell gene expression.[87,90] Some previous work has also been done and showed that AgNPs green synthesized by ethnic herbs have a role in scavenging free radicals and inhibiting the growth of various types of cancer cells.[90,91]

4. Conclusion

We have developed a unique, green, easy, rapid, efficient, and environmentally friendly solution plasma approach to prepare AgNPs using the extracts from *P. trimera* as a reduction agent. The formation of AgNPs with the presence of possible functional groups was demonstrated by UV-Vis and FTIR spectroscopy. The prepared AgNPs having an average size of about 8 nm showed high stability, good dispersion and high antibacterial and anticancer activities. The cytotoxicity against the gastric cancer cell line AGS and bactericidal activity against *S. aureus* and *P. aeruginosa* of the prepared AgNPs has been successfully demonstrated by the agar well diffusion method. The proposed approach may be appealing for the large-scale production of AgNPs for potential applications, especially in the ecologic nanoparticles in their bactericidal activity.

Conflicts of interest

The authors declare no possible conflict of interests.

Acknowledgements

This research was supported by Project of the TNU-University of Sciences in Vietnam under Grant number CS2021-TN06-15.

References

1 N. Hossain, M. A. Islam and M. A. Chowdhury, *Heliyon*, 2022, **8**, e12313.
2 A. Ahmed, M. Usman, Z. Ji, M. Rafiq, B. Yu, Y. Shen and H. Cong, *Mater. Today Chem.*, 2023, **27**, 101339.
3 H. D. Beyene, A. A. Werkneh, H. K. Bezabh and T. G. Ambaye, *Sustainable Mater. Technol.*, 2017, **13**, 18–23.
4 A. Shyam, S. Chandran, B. George and E. Sreelekha, *Inorg. Nano-Met. Chem.*, 2021, **51**, 1646–1662.
5 D. Sharma, S. S. Gulati, N. Sharma and A. Chaudhary, *Emergent Mater.*, 2021, **5**, 1649–1678.
6 A. Naganthran, G. Verasoundarapandian, F. E. Khalid, M. J. Masarudin, A. Zulkharnain, N. M. Nawawi, M. Karim, C. A. C. Abdullah and S. A. Ahmad, *Materials*, 2022, **15**, 427.
7 K. Alaqad and T. A. Saleh, *J. Environ. Anal. Toxicol.*, 2016, **6**, 384.
8 S. Gold and P. Nanoparticles, A Chemical Tool for Biomedical Applications, *Front. Chem.*, 2020, **8**, 376.
9 M. Guzman, J. Dille and S. Godet, *Nanomedicine*, 2012, **8**, 37–45.
10 S. Ahmed, M. Ahmad, B. L. Swami and S. Ikram, *J. Adv. Res.*, 2016, **7**, 17–28.
11 M. C. Sportelli, M. Izzi, A. Volpe, M. Clemente, R. A. Picca, A. Ancona, P. M. Lugarà, G. Palazzo and N. Cioffi, *Antibiotics*, 2018, **7**, 67.
12 D. T. Thuc, T. Q. Huy, L. H. Hoang, B. C. Tien, P. van Chung, N. T. Thuy and A. T. Le, *Mater. Lett.*, 2016, **181**, 173–177.
13 U. Shuaib, T. Hussain, R. Ahmad, M. Zakaullah, F. E. Mubarik, S. T. Muntaha and S. Ashraf, *Mater. Res. Express*, 2020, **7**, 035015.

14 T. Yoshida, N. Yamamoto, T. Mizutani, M. Yamamoto, S. Ogawa, S. Yagi, H. Nameki and H. Yoshida, *Catal. Today*, 2018, **303**, 320–326.
15 N. van Hao, N. van Dang, N. N. Anh, D. H. Tung, N. van Tu, B. H. Thang, P. N. Minh and P. van Trinh, *Mater. Lett.*, 2021, **287**, 129316.
16 N. van Hao, N. van Dang, D. H. Tung, P. T. Tan, N. van Tu and P. van Trinh, *RSC Adv.*, 2020, **10**, 41237–41247.
17 J. Patel, L. Němcová, P. Maguire, W. G. Graham and D. Mariotti, *Nanotechnology*, 2013, **24**, 245604.
18 T. Habib, J. M. A. Caiut and B. Caillier, *Nanotechnology*, 2022, **33**, 325603.
19 B. Bethi, S. H. Sonawane, B. A. Bhanvase and S. P. Gumfekar, *Chem. Eng. Process.*, 2016, **109**, 178–189.
20 Y. Oka, T. Kuroshima, K. Sawachika, M. Yamashita, M. Sakao, K. Ohnishi, K. Asami and M. Yatsuzuka, *Vacuum*, 2019, **167**, 530–535.
21 P. Rumbach and D. B. Go, *Top. Catal.*, 2017, **60**, 799–811.
22 A. Hussain, A. Mehmood, G. Murtaza, K. S. Ahmad, A. Ulfat, M. F. Khan and T. S. Ullah, *Green Process. Synth.*, 2020, **9**, 451–461.
23 J. Singh, T. Dutta, K. H. Kim, M. Rawat, P. Samddar and P. Kumar, *J. Nanobiotechnol.*, 2018, **16**, 1–24.
24 M. Tariq, K. N. Mohammad, B. Ahmed, M. A. Siddiqui and J. Lee, *Molecules*, 2022, **27**, 4754.
25 N. Ahmad, S. Sharma, M. K. Alam, V. N. Singh, S. F. Shamsi, B. R. Mehta and A. Fatma, *Colloids Surf., B*, 2010, **81**, 81–86.
26 N. Ahmad, S. Sharma, V. N. Singh, S. F. Shamsi, A. Fatma and B. R. Mehta, *Biotechnol. Res. Int.*, 2011, **2011**, 1–8.
27 S. Ahmed, Saifullah, M. Ahmad, B. L. Swami and S. Ikram, *J. Radiat. Res. Appl. Sci.*, 2016, **9**, 1–7.
28 B. Ajitha, Y. Ashok Kumar Reddy and P. S. Reddy, *Spectrochim. Acta, Part A*, 2014, **121**, 164–172.
29 N. I. S. B. Abdullah, M. B. Ahmad and K. Shameli, *Chem. Cent. J.*, 2015, **9**, 61.
30 W. A. Shaikh, S. Chakraborty, G. Owens and R. U. Islam, *Appl. Nanosci.*, 2021, **11**, 2625–2660.
31 A. Biosynthesis, L. Liotta, V. La Parola, A. Zuhrotun, D. Jihan Oktaviani and A. Nur Hasanah, *Molecules*, 2023, **28**, 3240.
32 G. M. Sulaiman, W. H. Mohammed, T. R. Marzoog, A. A. A. Al-Amiery, A. A. H. Kadhum and A. B. Mohamad, *Asian Pac. J. Trop. Biomed.*, 2013, **3**, 58–63.
33 S. M. Abu Nayem, N. Sultana, M. A. Haque, B. Miah, M. M. Hasan, T. Islam, M. M. Hasan, A. Awal, J. Uddin, M. A. Aziz and A. J. Saleh Ahammad, *Molecules*, 2020, **25**, 4773.
34 V. Nguyen, *J. Cancer Res. Ther.*, 2021, **17**, 471–476.
35 N. T. T. Le, D. H. Nguyen, N. H. Nguyen, Y. C. Ching, D. Y. P. Nguyen, C. Q. Ngo, H. N. T. Nhat and T. T. H. Thi, *Appl. Sci.*, 2020, **10**, 2505.
36 N. Rani, R. K. Singla, R. Redhu, S. Narwal, Sonia and A. Bhatt, *Curr. Top. Med. Chem.*, 2022, **22**, 1460–1471.
37 B. G. Ershov, E. Janata and A. Henglein, *J. Phys. Chem.*, 1993, **97**, 339–343.
38 R. Subramanian, P. Subbramaniyan and V. Raj, *Springerplus*, 2013, **2**, 1–11.
39 S. S. Shankar, A. Ahmad and M. Sastry, *Biotechnol. Prog.*, 2003, **19**, 1627–1631.
40 S. S. Shankar, A. Ahmad, R. Pasricha and M. Sastry, *J. Mater. Chem.*, 2003, **13**, 1822–1826.
41 G. Berhault, M. Bausach, L. Bisson, L. Becerra, C. Thomazeau and D. Uzio, *J. Phys. Chem. C*, 2007, **111**, 5915–5925.
42 A. Gole and C. J. Murphy, *Chem. Mater.*, 2004, **16**, 3633–3640.
43 W. Abdussalam-Mohammed, L. Mohamed, M. S. Abraheem, M. M. A. Mansour and A. M. Sherif, *Chemistry*, 2023, **5**, 54–64.
44 P. Rani, V. Kumar, P. P. Singh, A. S. Matharu, W. Zhang, K. H. Kim, J. Singh and M. Rawat, *Environ. Int.*, 2020, **143**, 105924.
45 N. Liaqat, N. Jahan, Khalil-ur-Rahman, T. Anwar and H. Qureshi, *Front. Chem.*, 2022, **10**, 995.
46 S. Khan, S. Singh, S. Gaikwad, N. Nawani, M. Junnarkar and S. V. Pawar, *Environ. Sci. Pollut. Res.*, 2020, **27**, 27221–27233.
47 S. Jain and M. S. Mehata, *Sci. Rep.*, 2017, **7**, 1–13.
48 M. I. Masum, M. M. Siddiqa, K. A. Ali, Y. Zhang, Y. Abdallah, E. Ibrahim, W. Qiu, C. Yan and B. Li, *Front. Microbiol.*, 2019, **10**, 820.
49 L. Castro, M. L. Blázquez, J. A. Muñoz, F. González and A. Ballester, *IET Nanobiotechnol.*, 2013, **7**, 109–116.
50 C. Miron, M. A. Bratescu, N. Saito and O. Takai, *Plasma Chem. Plasma Process.*, 2010, **30**, 619–631.
51 P. Pootawang, N. Saito, O. Takai and S. Y. Lee, *Nanotechnology*, 2012, **23**, 395602.
52 G. Bagherzade, M. M. Tavakoli and M. H. Namaei, *Asian Pac. J. Trop. Biomed.*, 2017, **7**, 227–233.
53 N. E. A. El-Naggar, M. H. Hussein, S. A. Shaaban-Dessuuki and S. R. Dalal, *Sci. Rep.*, 2020, **10**, 1–19.
54 M. Ali, B. Kim, K. D. Belfield, D. Norman, M. Brennan and G. S. Ali, *Mater. Sci. Eng., C*, 2016, **58**, 359–365.
55 Z. Salari, F. Danafar, S. Dabaghi and S. A. Ataei, *J. Saudi Chem. Soc.*, 2016, **20**, 459–464.
56 P. Mukherjee, M. Roy, B. P. Mandal, G. K. Dey, P. K. Mukherjee, J. Ghatak, A. K. Tyagi and S. P. Kale, *Nanotechnology*, 2008, **19**, 075103.
57 M. Kgatshe, O. S. Aremu, L. Katata-Seru and R. Gopane, *J. Nanomater.*, 2019, **2019**, 3501234.
58 X. Hou and Y. Fang, *J. Colloid Interface Sci.*, 2007, **316**, 19–24.
59 N. Biswas, S. Kapoor, H. S. Mahal and T. Mukherjee, *Chem. Phys. Lett.*, 2007, **444**, 338–345.
60 J. Chowdhury and M. Ghosh, *J. Colloid Interface Sci.*, 2004, **277**, 121–127.
61 A. J. Kora, R. B. Sashidhar and J. Arunachalam, *Carbohydr. Polym.*, 2010, **82**, 670–679.
62 M. Khan, M. Khan, S. F. Adil, M. N. Tahir, W. Tremel, H. Z. Alkhathlan, A. Al-Warthan and M. R. H. Siddiqui, *Int. J. Nanomed.*, 2013, **8**, 1507–1516.
63 K. Anandalakshmi, J. Venugobal and V. Ramasamy, *Appl. Nanosci.*, 2016, **6**, 399–408.
64 M. Behravan, A. Hossein Panahi, A. Naghizadeh, M. Ziaee, R. Mahdavi and A. Mirzapour, *Int. J. Biol. Macromol.*, 2019, **124**, 148–154.

65 S. Chen and K. Kimura, *J. Phys. Chem. B*, 2001, **105**, 5397–5403.
66 P. Magudapathy, P. Gangopadhyay, B. K. Panigrahi, K. G. M. Nair and S. Dhara, *Phys. B*, 2001, **299**, 142–146.
67 A. Gole and C. J. Murphy, *Chem. Mater.*, 2004, **16**, 3633–3640.
68 C. Miron, M. A. Bratescu, N. Saito and O. Takai, *Plasma Chem. Plasma Process.*, 2010, **30**, 619–631.
69 C. Chokradjaroen, X. Wang, J. Niu, T. Fan and N. Saito, *Mater. Today Adv.*, 2022, **14**, 100244.
70 P. Pootawang, N. Saito, O. Takai and S. Y. Lee, *Nanotechnology*, 2012, **23**, 395602.
71 S. Zaima, M. Sase, H. Adachi and Y. Shibata, *J. Phys. D: Appl. Phys.*, 1978, **11**, L179.
72 A. Nel, T. Xia, L. Mädler and N. Li, *Science*, 2006, **311**, 622–627.
73 G. Bhumi, R. M. Linga and N. Savithramma, *Asian J. Pharm. Clin. Res.*, 2015, **8**, 62–67.
74 H. S. Uhm, J. H. Kim and Y. C. Hong, *Phys. Plasmas*, 2007, **14**, 073502.
75 D. Meroni and S. Ardizzone, *Nanomaterials*, 2018, **8**, 891.
76 E. O. Mikhailova, *J. Funct. Biomater.*, 2020, **11**, 84.
77 M. J. Ahmed, G. Murtaza, A. Mehmood and T. M. Bhatti, *Mater. Lett.*, 2015, **153**, 10–13.
78 M. R. Bindhu and M. Umadevi, *Spectrochim. Acta, Part A*, 2014, **128**, 37–45.
79 R. S. Patil, M. R. Kokate and S. S. Kolekar, *Spectrochim. Acta, Part A*, 2012, **91**, 234–238.
80 S. Naraginti and A. Sivakumar, *Spectrochim. Acta, Part A*, 2014, **128**, 357–362.
81 I. Sondi and B. Salopek-Sondi, *J. Colloid Interface Sci.*, 2004, **275**, 177–182.
82 J. R. Morones, J. L. Elechiguerra, A. Camacho, K. Holt, J. B. Kouri, J. T. Ramírez and M. J. Yacaman, *Nanotechnology*, 2005, **16**, 2346.
83 S. Ahmed, M. Ahmad, B. L. Swami and S. Ikram, *J. Adv. Res.*, 2016, **7**, 17–28.
84 S. Salehi, S. A. Sadat Shandiz, F. Ghanbar, M. R. Darvish, M. S. Ardestani, A. Mirzaie and M. Jafari, *Int. J. Nanomed.*, 2016, **11**, 1835–1846.
85 M. A. Ebrahimzadeh, Z. Hashemi, M. Mohammadyan, M. Fakhar and S. Mortazavi-Derazkola, *Surf. Interfaces*, 2021, **23**, 100963.
86 S. Aslany, F. Tafvizi and V. Naseh, *Mater Today Commun.*, 2020, **24**, 101011.
87 R. A. Hamouda, M. H. Hussein, R. A. Abo-Elmagd and S. S. Bawazir, *Sci. Rep.*, 2019, **9**, 13071.
88 T. Xia, M. Kovochich, J. Brant, M. Hotze, J. Sempf, T. Oberley, C. Sioutas, J. I. Yeh, M. R. Wiesner and A. E. Nel, *Nano Lett.*, 2006, **6**, 1794–1807.
89 M. F. Rahman, J. Wang, T. A. Patterson, U. T. Saini, B. L. Robinson, G. D. Newport, R. C. Murdock, J. J. Schlager, S. M. Hussain and S. F. Ali, *Toxicol. Lett.*, 2009, **187**, 15–21.
90 R. Vivek, R. Thangam, K. Muthuchelian, P. Gunasekaran, K. Kaveri and S. Kannan, *Process Biochem.*, 2012, **47**, 2405–2410.
91 I. A. Radini, N. Hasan, M. A. Malik and Z. Khan, *J. Photochem. Photobiol., B*, 2018, **183**, 154–163.